

Stored energy release in neutron irradiated silicon carbide

Lance L. Snead ^{a, b}, Yutai Katoh ^c, Takaaki Koyanagi ^c, Kurt Terrani ^c

^a Massachusetts Institute of Technology, Cambridge, MA, USA

^b Stony Brook University, Stony Brook, NY, USA

^c Oak Ridge National Laboratory, Oak Ridge, TN, USA

Abstract

The purpose of this investigation is to experimentally quantify the stored energy release upon thermal annealing of previously irradiated high-purity silicon carbide (SiC.) Samples of highly-faulted polycrystalline CVD b-SiC and single crystal 6H-SiC were irradiated in a mixed spectrum fission reactor near 60 °C in a fluence range from 5×10^{23} to 2×10^{26} n/m² ($E > 0.1$ MeV), or about 0.05-20 dpa, in order to quantify the stored energy release and correlate the release to the observed microscopic swelling, lattice dilation, and microstructure as observed through TEM. Within the fluence of this study the crystalline material was observed to swell to a remarkable extent, achieving 8.13% dilation, and then cross a threshold dose for amorphization at approximately 1×10^{25} n/m² ($E > 0.1$ MeV) Once amorphized the material attains an as-amorphized swelling of 11.7% at this irradiation condition. Coincident with the extraordinary swelling obtained for the crystalline SiC, an equally impressive stored energy release of greater than 2500 J/g at the critical threshold for amorphization is inferred. As expected, following amorphization the stored energy in the structure diminishes, measured to be approximately 590 J/g. Generally, the findings of stored energy are consistent with existing theory, though the amount of stored energy given the large observed crystalline strain is remarkable. The overall conclusion of this work finds comparable stored energy in SiC to that of nuclear graphite, and similar to graphite, a stored energy release in excess of its specific heat in some irradiation conditions.

1. Introduction

Throughout 1943 the Metallurgical Project at the University of Chicago and in particular the Theoretical Physics Group were deeply involved in developing the fundamental physics supporting construction of the first plutonium-producing graphite reactor. During that time, and in the same report where the first nuclear chain reaction was described [1], Eugene Wigner also suggested the possibility of substantial fast-neutron damage to materials. This damage, in the form of displacement of atoms from their original lattice positions, became known as the “Wigner Effect.” Following this, a range of theoretical and experimental work was carried out on nuclear graphite to determine the expected changes in physical dimensions, thermal and electrical conductivity, and stored energy due to the Wigner Effect. This last property, the amount of energy retained in the defected structure, was first postulated by Szilard [2] to have significant implications in the event of release. The stored energy release then became known as the “Szilard Complication.”

Energy stored in and subsequently released upon the annealing of the defected structures of neutron-damaged materials is a universal phenomenon, although the amount and impact of its release is strongly material and irradiation temperature dependent. The most widely studied and technologically important material displaying this phenomenon is nuclear graphite, which can release on the order of a few kJ's/g. For perspective, this amount greatly exceeds current battery storage technologies whose energy release ranges from ~ 0.04 kJ/g for lead-acid batteries to ~ 0.5 kJ/g for lithium ion batteries. For graphite, as with most nuclear materials, simple defect production and annihilation dominate stored energy. As shown in Fig. 1, a saturation level for stored energy occurs that is quite irradiation temperature dependent, as the graphite microstructure makes a transition from a regime of single interstitial-vacancy pairs or very simple cluster production (dominating below approximately 150 °C) to one in which larger vacancy loops and more complex defects dominate [3].

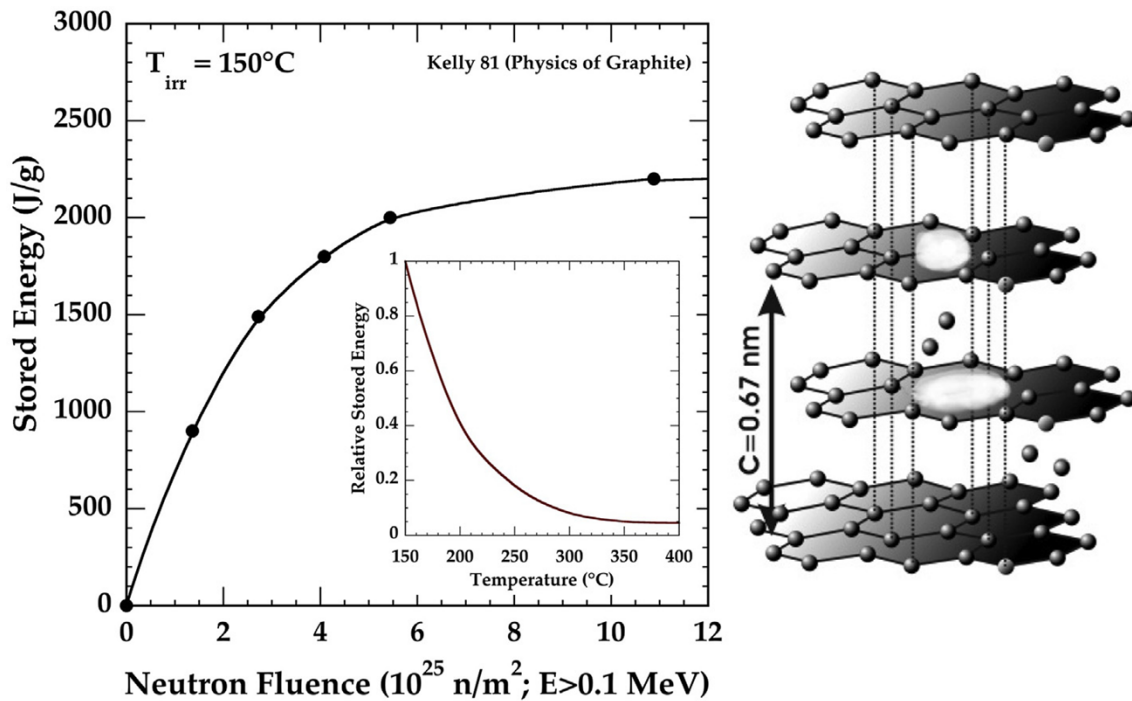


Fig. 1. Stored energy in nuclear graphite (crystal depicted to right) with inset relative stored energy as a function of irradiation temperature replotted from Kelly [7]. Below a few hundred Celsius, stored energy release is dominated by recovery of simple interstitial-vacancy complexes or annihilation of simple clusters. Note: Fluence units have been converted from original EDN: $\times 10^{21}$ n/cm² to n/m² ($E > 0.1$ MeV) using a conversion factor of 1.36.

While stored energy has been understood to exist in a range of materials, only sporadic (though in many cases detailed) studies have been carried out on non-graphite materials. However, it is noted that in an early work comparing the stored energy of graphite to diamond Primak [4,5] noted the possibility of appreciable stored energy (suggesting ~ 418 J/g) in SiC irradiated near 30 °C to relatively low neutron fluence of 4.3×10^{23} n/m² ($E > 75$ eV) in the Hanford Pile, though apparently did not publish further in the area. Recently, the present authors [6] noted an extraordinary level

of swelling (7.8%) for neutron irradiated SiC prior to the material's transition to the amorphous state. Given this apparent high level of defect concentration combined with an understanding of the vacancy and interstitial formation energies of SiC it was postulated that stored energy release in excess of material specific heat existed suggesting the possibility of autocatalytic reactions under certain conditions. The goal of this work is to provide initial data into the stored energy of SiC.

2. Experimental

The material for this work was ultra-high purity highly-faulted polycrystalline CVD SiC produced by Rohm & Haas Advanced Materials (presently a subsidiary of Dow Chemical, Woburn, MA.) The single crystal material was electronic grade 6HeSiC procured from Cree. Sample. Irradiation was carried out in the mixed neutron spectrum hydraulic tube, or peripheral target tube positions of the High Flux Isotope Reactor (HFIR.) Irradiation capsule configuration was of an aluminum tube with perforated walls through which HFIR coolant water passed and contacted the sample holders. The sample holders consisted of thinly wrapped laser-welded aluminum foil packets containing the SiC. The HFIR coolant water enters the core at 49 °C and exits at 69 °C. Samples were located mid-core such that the exterior of the sample-wrap should be ~60 °C. Samples were irradiated at (0.02, 0.1, 0.5, 0.762, 1.34, 2, and 20) $\times 10^{25}$ n/m² (E > 0.1 MeV) The fast neutron flux in this position of HFIR was approximately 1×10^{19} n/m²-s (E > 0.1 MeV) corresponding to approximately 10^{-6} dpa/s. The fluence is calculated based on the known flux in the irradiation position and the elapsed irradiation time. It is considered accurate within a few percent. For this paper an equivalence of 1×10^{25} n/m² (E > 0.1 MeV) = 1 displacement per atom (dpa) is assumed. The majority of samples were square, approximately 6mm on edge and 2.8mm thick. While the nuclear heating of the HFIR is extraordinarily high, given the relatively thin sample geometry the temperature gradient (difference between surface and centerline temperature) is less than a few degrees Celsius.

Once samples were removed from their irradiation capsules they were ultrasonically cleaned first with ethyl alcohol and then immersed in hydrofluoric acid for approximately 30 minutes in order to remove any glassy film present. Both density through density gradient column (DGC) and as-inferred through lattice dilation (x-ray diffraction) was determined. The DGC utilized mixtures of methylene iodide and tetrabromomethane in a column of approximately 1m in height yielding a density gradient of 0.002 (g/cm³) per centimeter of column length. Calibrated floats were used to ensure column linearity and interpolate sample density. A temperature correction was used per ATSM guideline ASTM D1505-18. More detail on the DGC as applied to a subset of these specimens can be found elsewhere [6]. The error associated with the density measurement, assuming no sample surface contamination, is less than 0.001 g/cm³, or < 0.03%.

Lattice constant measurement of the irradiated specimens before and after annealing (release of stored energy) was conducted. The results of the as-irradiated specimens have already been reported [6] with some of the data re-reported here for clarity. In order to carry out x-ray analysis samples were wrapped in Kapton foil for contamination control prior to placing in a Bruker D2 Phaser (30 kV, 30 mA) with Cu Ka radiation. An internal Si standard (NIST SRM640d) was used for calibration of peak positions. The Bragg center of reflection was found by least-squares fitting

to a Gaussian profile. Lattice parameters were determined by least-squares refinement of angles calculated using Bragg's law to measured Bragg angles.

Transmission Electron Microscopy (TEM) in this work was performed on focus ion beam prepared (FEI-Versa 3D Dual Beam operated at 30 KeV) samples. A finish mill at 2e5 KeV was applied. A JEM2100F operating at 200 kV was used for the TEM imaging. The same procedure was carried out in the previous work [6].

Stored energy measurements were carried out for the specimens cleaned with hydrofluoric acid using a Netzsch DSC 404C Thermal Analyzer. For these measurements a three step process to determine the stored energy was utilized: 1) Run the system to temperature under argon gas to temperature to calibrate system with both sample and reference Pt pans empty. 2) Run the sample pan with a standard sapphire sample and the reference pan empty to obtain correlation between DSC signal and known heat capacity, and 3) Run irradiated sample in the sample pan with reference pan empty to determine the stored energy release by comparison with (2). This calibration process was conducted for every 2-3 specimens. The heating rate was set to be 20 °C/min. The basic test procedure followed ASTM E1269-11. The maximum test temperature was 700 °C. It was confirmed that there was no notable reaction among specimens and Pt pan after the measurement. Through repeated, individual measurement and comparison to the known specific heat of SiC the run-to-run accuracy was seen to be $\pm 3\%$ with resulting stored energy release accuracy of $\pm 5\text{-}6\%$.

3. Results

Figs. 2 and 3 provide summary plots of the raw data-curves as generated by the scanning calorimeter and in the reduced form of stored energy accumulation in comparison with swelling. In Fig. 2 the calorimetry has been carried out on each sample in the as-irradiated condition and subsequent to this nominal 700 °C anneal, in the as-annealed condition. The latter measurement was carried out to ensure the sample did not liberate any further heat, thus mimicking a non-irradiated CVD SiC sample, which was shown to be the case. It is emphasized that the temperature measured in this experiment was within the cup of the calorimeter and is therefore the proscribed ramp temperature. It would be expected that the actual sample temperature would increase when the energy release exceeded the sample specific heat. As will be shown, this was the case for the higher dose specimens. Moreover, as evidenced by Fig. 2 (and specifically the DCS output for the 0.5 dpa sample during the ramp-up in temperature), while the kinetics of release are not precisely determined in this experiment, the heat release is occurring over a period of minutes.

The amount of swelling recovery of the same samples following their measurement (annealing) during the stored energy measurement is provided in Fig. 3. Here swelling recovery is defined as the percent original swelling that has been annealed-out following the 700 °C maximum temperature achieved during the stored energy measurement. The as-irradiated swelling data includes data previously reported [6] as well as new data whose purpose was to narrow the uncertainty in the amorphous transition point (the 0.762 and $1.34 \times 10^{25} \text{ n/m}^2$, $E > 0.1 \text{ MeV}$ data.) The amorphous transition point is simply approximated as the intersection of the as-irradiated swelling trend line for the crystalline material and the as-amorphized line. At this irradiation temperature the approximate dose of $1 \times 10^{25} \text{ n/m}^2$ is suggested as the amorphous transition. In both as-irradiated and as-annealed (700 °C recovered) state swelling as determined through x-ray

diffraction lattice strain agrees well (essentially is identical) with DCG bulk density, as indicated by overlapping data points on Fig. 3.

The accumulation of stored energy prior to the point of amorphization, within the limited data of the study, appears to accumulate in a linear fashion. This linear accumulation occurs at least to the highest dose for which the SiC is known to remain crystalline ($0.762 \times 10^{25} \text{ n/m}^2$, $E > 0.1 \text{ MeV}$) In Fig. 3 two as amorphized samples of approximately equivalent density are also presented each indicating large, though significantly lower stored energies than the material possessed near the critical amorphization threshold, consistent with the structure transitioning to a lower energy state. Fig. 4 provides a high-resolution TEM image of a single crystal 6H SiC that has undergone 7.7% swelling, clearly indicating the presence of a highly faulted crystalline structure and a diffraction pattern consistent with a highly strained crystalline lattice. X-ray diffraction on the highly faulted FCC and single crystal 6H-HCP materials irradiated from 0.5 to $1.34 \times 10^{25} \text{ n/m}^2$, $E > 0.1 \text{ MeV}$ support the conclusion that the material is in a highly strained crystalline condition. Close inspection of Fig. 4 suggests the potential for the onset and formation of discontinuous amorphous pockets in the material. At some level above this irradiation dose a phase transition to a completely amorphous structure is expected. The maximum stored energy release measured was at the 7.7% swelling point, yielding 1390 J/g. While a sample was irradiated to higher dose ($0.762 \times 10^{25} \text{ n/m}^2$ ($E > 0.1 \text{ MeV}$)) and remained in a crystalline condition with 8.13% strain, stored energy was not measured for that sample.

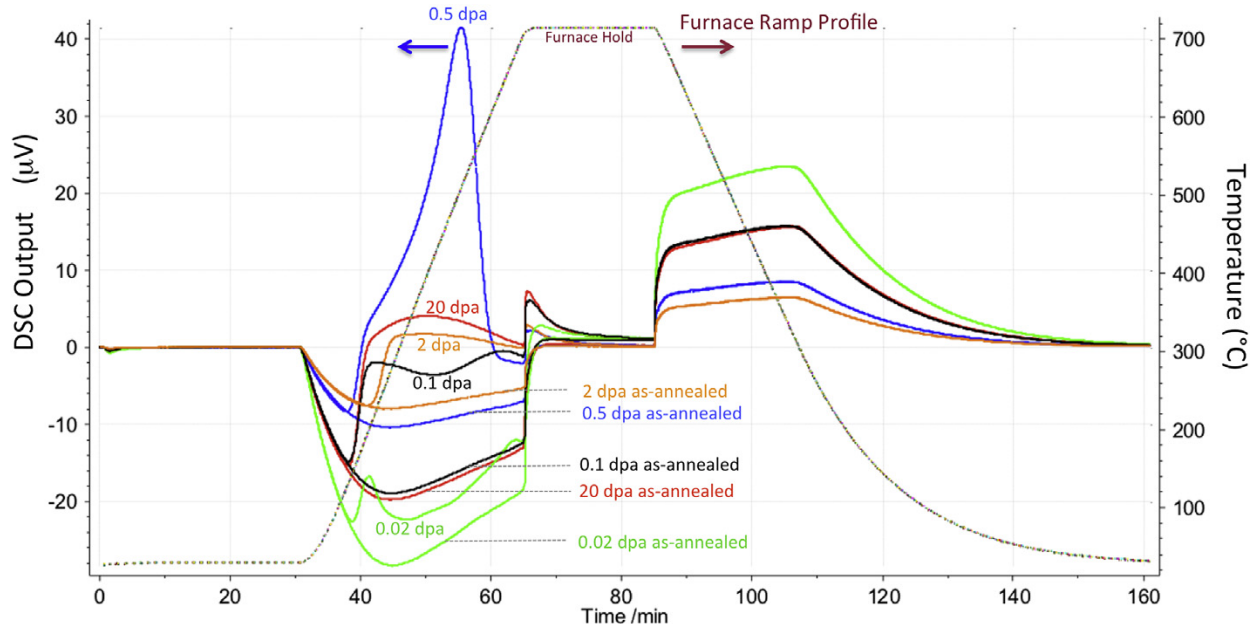
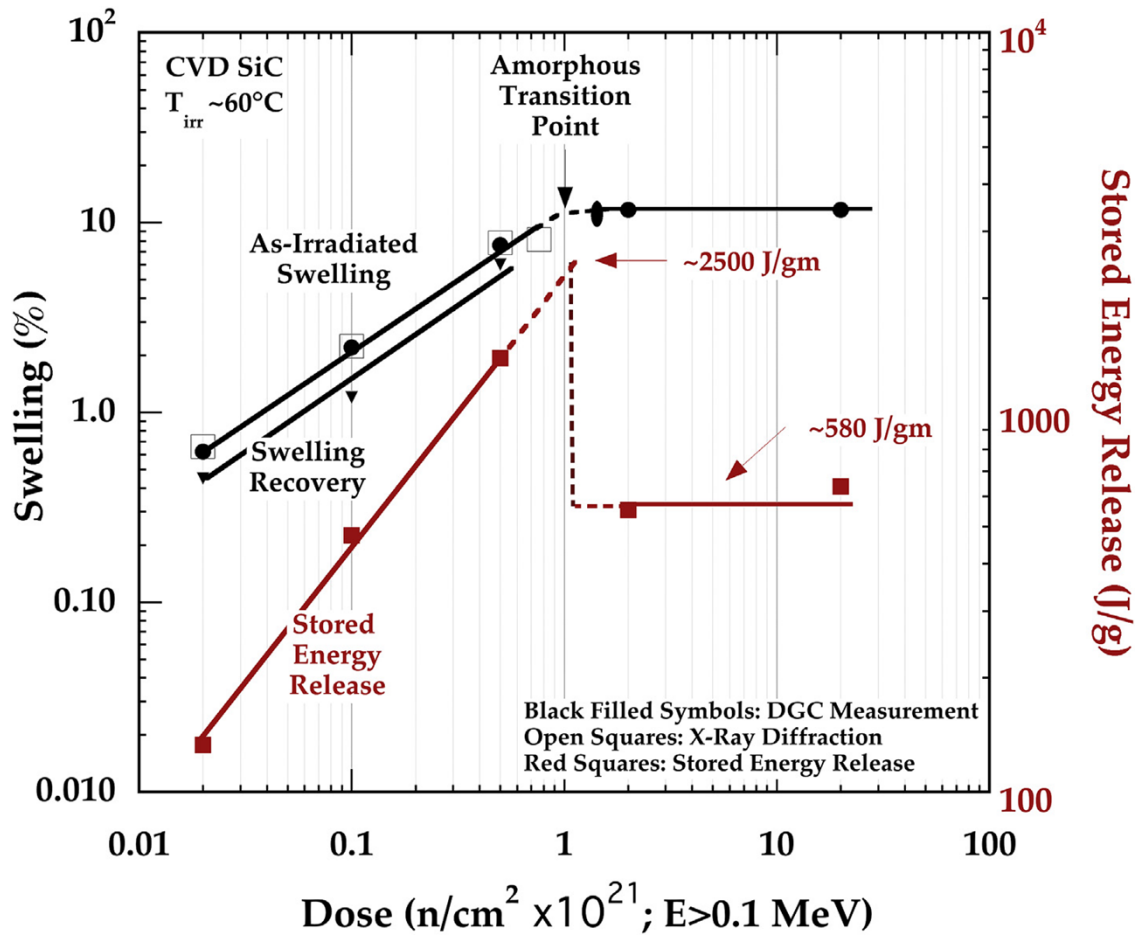


Fig. 2. Scanning calorimeter raw data curves.

The red dotted lines of Fig. 3 extrapolate the stored energy curved to the approximate point of maximum stored energy, assumed to exist just prior to the critical fluence for amorphization. The horizontal solid red line provides the stored energy of the two amorphized SiC samples, or a value of 580 J/g stored energy at this amorphization condition. Amorphization was confirmed through x-ray diffraction (see Fig. 5 below). Following annealing at 700 °C the density of the amorphized samples were not measured. However, it is known from the literature [8] that densification of the

amorphous structure occurs upon annealing above the irradiation temperature. In that work as-amorphized SiC was seen to densify monotonically by approximately 5% prior to reaching the recrystallization temperature of 885 °C at which point rapid recrystallization to non-irradiated density occurs. Unfortunately, the upper annealing temperature of this study (700 °C) was short of the SiC recrystallization temperature thus the samples remained in a relaxed amorphous state. Assuming similar annealing kinetics to the previous work [8] it is assumed that these amorphous samples would continue to densify by approximately 0.05% producing an additional ~290 J/g and then recrystallize.



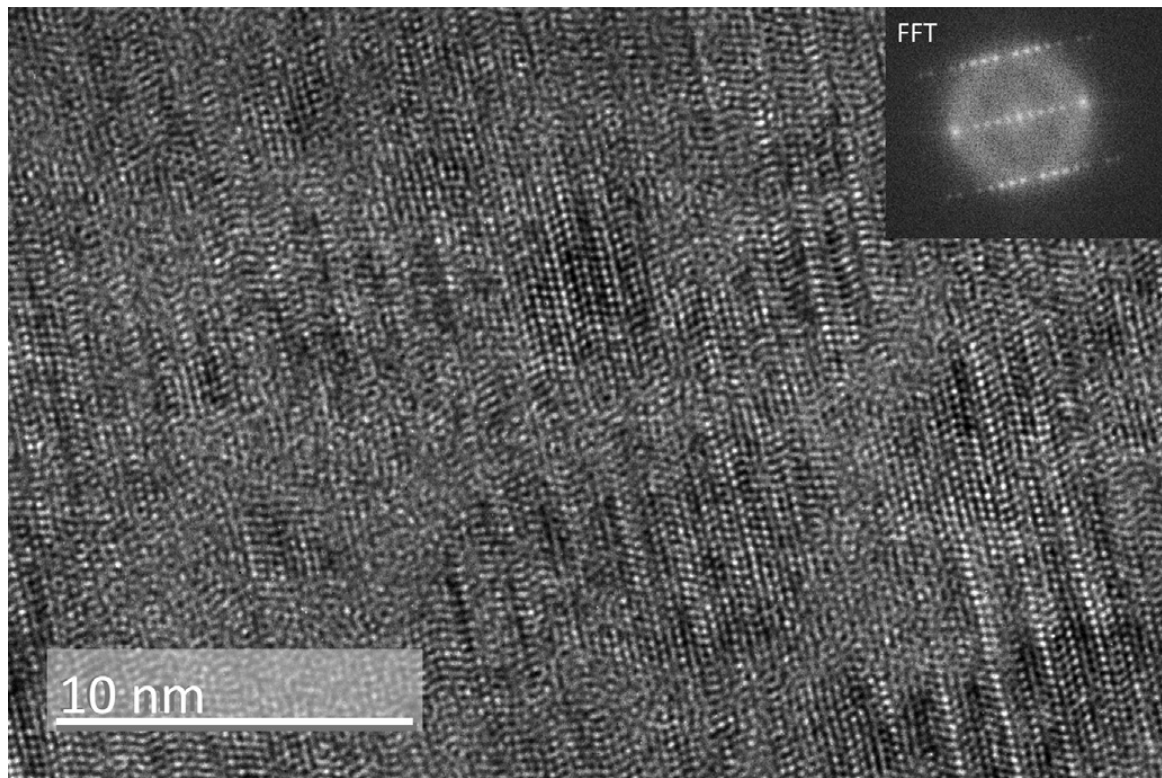


Fig. 4. TEM of highly faulted SiC undergoing 7.7% volume change.

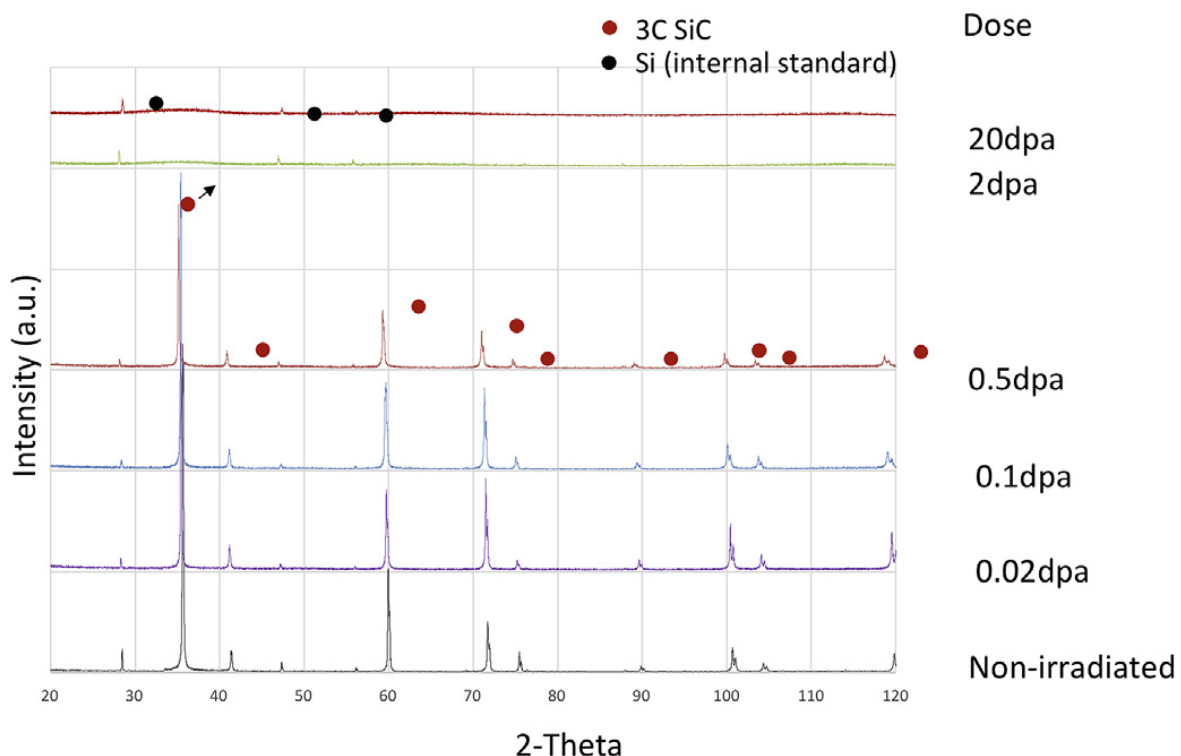


Fig. 5. X-ray diffraction of non-irradiated, faulted, and amorphous samples following 700 °C stored-energy measurement. Black and red dots refer to Si and SiC crystal peak standards utilized

in analysis. (For interpretation of the references to colour in this figure legend, the reader is referred to the Web version of this article.)

4. Discussion

The swelling, amorphization, and effects of annealing the as irradiated structure of SiC have been well studied and at this point are fairly well understood [9-24]. Stored energy release, while studied in detail in nuclear graphite due to its technological importance, has also been studied for a wide array of materials. Interestingly, following the first studies to reveal stored energy on graphite by Maurer and Ruder [25], the next material to be investigated for large neutron-irradiation-induced stored energy release was diamond, publishing [26] extreme energy release exceeding 600 J/g following annealing of fast neutron irradiation to ~ 0.06 dpa. However, prior to these first discussions of Wigner Energy there was related work on the self-damage, amorphization, and stored energy release of uranium and thorium-bearing crystals: the so called metamict state. In 1942 Faessler [27] reported on his discovery of 373 J/g energy release in the monoclinic mineral gadolinite $(Ce,La,Nd,Y)2FeBe2Si2O10$ with this damage and stored energy release suggested as a means of mineral dating [28]. Following this first finding a number of researchers demonstrated energy release in naturally radioactive minerals such as the ABO_4 and AB_2O_6 pyrochlores davydite [29], fergusonite [29e31], priorite [29], ellsworthite [30], sammarskite [28,31], euxenite [28,31], brannerite [31] and exchynite-priorite [30]. For these pyrochlores the energy release ranges from tens to a few hundred J/g. Zircons have also been shown to release as much as 322 J/g through their millennia of internal α -decay followed by laboratory annealing [32,33]. Beyond graphite and certain minerals the stored energy release has also been utilized to provide fundamental stage-I defect kinetics in neutron irradiated materials. The range of materials studied include solid Argon [34] providing 11.17 J/g, a range of low temperature metals such as Cu ($\sim 0.038\text{--}0.82$ J/g) [35e38], Si (10.4 J/g) [39,40], Magnesium (4.9 J/g) [41], Beryllium (3.4 J/g) [42], Aluminum (0.46 J/g) [43], Iron (~ 2 J/g) [44], Ni (~ 1.9 J/g) [44], Molybdenum (1.7 J/g) [45] and ceramics such as BeO [46e48] (8.4- $\text{--} 368$ J/g), MgO (19.8 J/g) [47,48], Al₂O₃ (117 J/g) [47-49] and UO₂ (104 J/g) [50] as well as nano-diamond (to >1500 J/g) [26,51] and a range of candidate nuclear waste form materials such as neutron irradiated silica and borosilicate glass (<150 J/g) [47-49].

Perhaps of significance in regards to the present work is the magnitude and kinetics of stored energy release in SiC. As with graphite, and as depicted in Fig. 6, the stored energy release for SiC can exceed its specific heat, potentially leading to an autocatalytic reaction depending on the specifics of the application. In Fig. 6 it is seen that the ~ 0.1 dpa irradiated and crystalline sample has moderately less stored energy release as compared to its specific heat in this 20 °C/min temperature ramp, while the stored energy release for the 0.5 dpa irradiated crystalline sample heated at the same ramp rate greatly exceeds the sample specific heat. Not plotted in the figure are the two amorphous samples, both of which exhibit stored energy release curves slightly in excess of the specific heat. As discussed in the introductory section, the presence of stored energy in SiC is to be expected, though its magnitude is impressive. Fig. 7 provides the SiC stored energy of the present study as a function of dose and in comparison with the range of the neutron irradiated materials discussed above. In all cases materials were irradiated in the low temperature regime (<0.3 Tm) consistent with limited interstitial mobility and simple point defect and cluster formation. In some cases the apparent saturation may be due to interstitial mobility. It is noted that caution regarding direct comparison of the data in Fig. 7 is warranted as these data span five

decades in time with variable precision in calorimetry and fluence determination. Moreover, while most data span an annealing range in which most of the defects would be expected to anneal, some experiments had an abbreviated range in annealing (i.e. as with the current study, not all of the stored energy was released.)

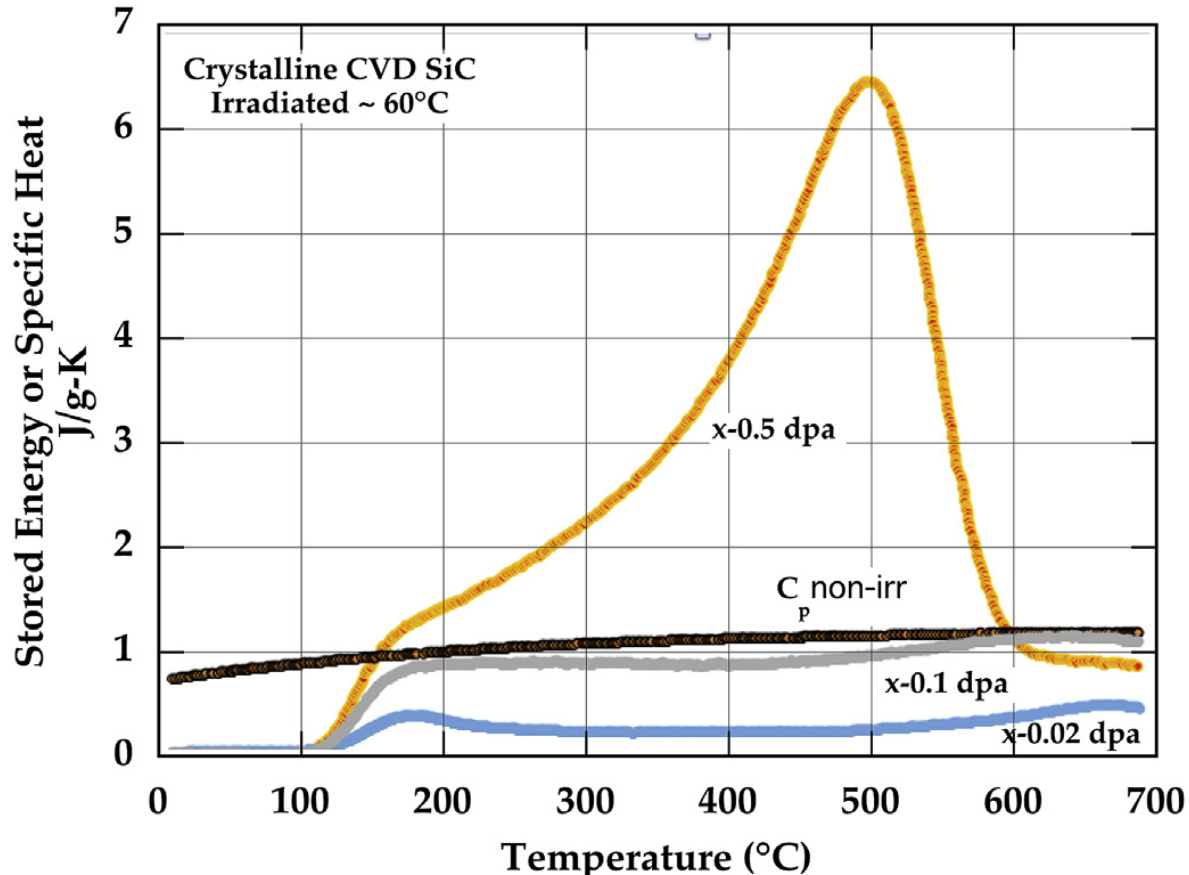


Fig. 6. Specific heat of non-irradiated and stored energy of crystalline SiC.

The data of Fig. 7 provide a number of general insights into stored energy, though relation to underlying defect structures responsible and defect kinetics is challenging. From the figure it is clear that SiC is accumulating stored energy at a rate greater than that of graphite and ultimately to levels on par with graphite. Moreover, Fig. 7 clearly supports the general tendency for strongly bonded covalent and ionic materials to store energy to higher levels than metals.

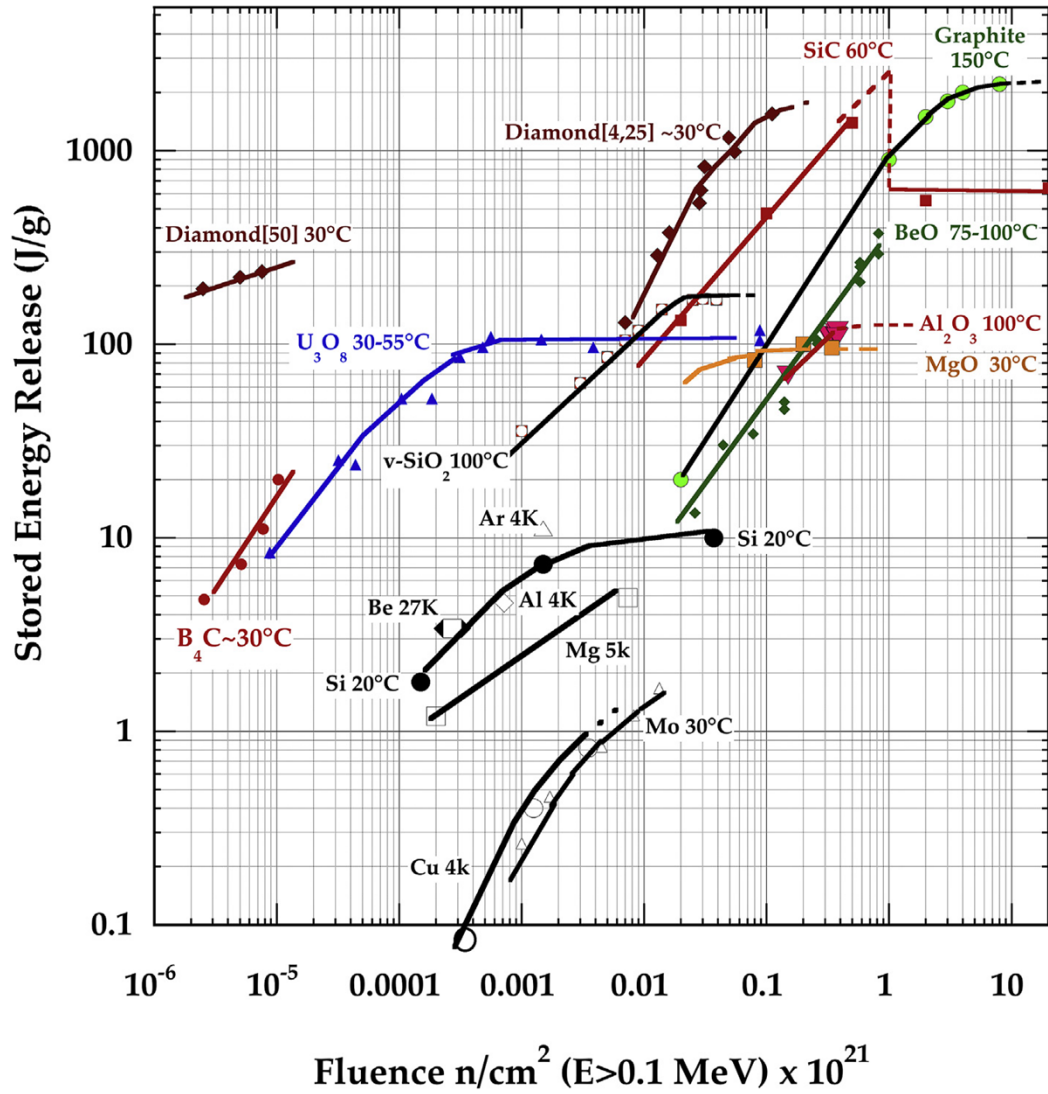


Fig. 7. Stored energy release of SiC as a function of dose as compared with a range of archival data.

Table 1
Estimated contributions of various point defects to swelling and stored energy.

	I_{Si}	I_C	V_{Si}	V_C	S_{Si}	C_{Si}	(Total)
Excess volume (\AA^3) [52]	27.9–37.2	15.3–16.5	1.9	2.7	15.4	-9.5	n/a
Defect Fraction estimated from Swaminathan [53]	3.5%	38.0%	8.4%	33.0%	11.0%	6.3%	~100%
Defect Fraction estimated from Gao and Weber [54]	-7%	-23%	-9%	-21%	-21%	-19%	100%
Contribution to swelling per Swaminathan [53]	-12%	-65%	-2%	-10%	-18%	-7%	100%
Estimated concentration at 1% swelling: $C_{1\%}$	-0.04%	-0.43%	0.10%	0.37%	0.12%	0.07%	1.13%
Formation Energy: E_f (eV)	8.754	6.953	4.966	4.193	3.564	4.034	n/a
Product of E_f and $C_{1\%}$ (J/g)	-17	-143	-23	-75	-21	-14	~293
Contribution to stored energy	-6%	-48%	-8%	-26%	-7%	-5%	100%

The detailed microstructural basis for energy storage and release in neutron irradiated SiC can only be speculated upon at this time: defects produced in SiC during the displacement cascade events include the Frenkel defects of both elements and two types antisites: ISi, IC, VSi, VC, SiC, and

CSi, isolated or clustered. At the temperature of this irradiation, only correlated recombination of CFrenkel pairs is expected to take place among various thermally activated defect recovery processes involving the above species. In other words, there should be no long-range migration of any of these defects. The excess volumes associated with these isolated defects have been previously calculated by Li and Porter [52] by molecular dynamics simulation using a Tersoff potential. Parsing the individual defects at 200 K has also been estimated by Swaminathan et al. [53] and Gao and Weber [54] in separate works. These data sets are presented in summary in Table 1 along with the estimated contributions to swelling from the various defect species based on the Swaminathan et al. results. Using the formation energy values for individual defects (as published by Shrader et al. [55] though noting that considerable variation exists for the defect formation energy values as discussed in the literature [56-59]), contributions from various defect species to the stored energy may be estimated. The result indicates that the majority (~74%) of stored energy is due to C-Frenkel defects while the remainder is about equally shared by the Si-Frenkel defects and the antisite defects.

As noted, the Table 1 analysis is based on the defect partitioning as presented by the Swaminathan et al. Were the Gao-Weber formalism utilized the results would not significantly different, though a slight reduction to the C-Frenkel defect contribution and an increased antisite contribution would take place. The gradual stored energy release against temperature during the calorimetry runs, instead of a sharp release at the Stage II recovery temperature, is attributed to the gradual IC clustering due to the energy barrier for IC-VC recombination. It should be noted that this (Table 1) exercise involves significant assumptions (such as isolation of all defects) and is only intended to provide a rough estimate of the fractional contributions of various defects to the total stored energy. Regardless, the measured stored energy at 1% swelling (~221 J/g) appears to be in general agreement with the total energy released as provided in Table 1 (~293 J/g). Moreover, closer agreement would be expected as the 700 °C anneal of this work (cf Fig. 2) liberated on the order of 72% of the irradiation induced lattice strain (i.e. the expected stored energy for complete recovery would be closer to 300 J/g.)

Regarding the magnitude of stored energy in relation to the critical amorphization threshold, a number of authors [60-62] have considered as the defining point of material amorphization the point when the cumulative defect energies of the material becomes equal to the energy differential (DEam) between the crystalline and amorphous phases. In the SiC system DEam has been estimated through various experimental and modeling activities in the range from 0.6 to 2 eV with associated energy densities in SiC of 1470-4900 J/g. Here the maximum measured stored energy was in reasonable agreement at ~1390 J/g, extrapolated to ~2500 J/g at the assumed amorphization dose of $\sim 1 \times 10^{25} \text{ n/m}^2$, $E > 0.1 \text{ MeV}$. As a side-note the authors would like to emphasize that this so-called critical point for amorphization is known to be a function of temperature [14,16,63-68] and irradiating species [14-17,66-69] and a relatively weaker function of the dose rate [15,64,70]. As such, the critical point for amorphization is known to vary substantially in the literature. Setting aside any issues with respect to assumption of sublattice displacement energies used to calculate dpa (i.e., as used in the SRIM calculations in the literature), the assumed 1 dpa value of critical amorphization threshold put forward here is consistent with 1) the lower mass energetic ions causing the damage [14,16,63-68] (subcascades produced by neutron irradiation), and 2) lower damage rate of neutron irradiation as compared to the ion irradiation in the literature [15]. Both of these factors act to increase the critical amorphization threshold.

Finally, it is pointed out that the irradiation temperature of this campaign, ~ 60 $^{\circ}\text{C}$, is very low with respect to currently proposed nuclear applications of SiC and therefore care must be taken when extrapolating results to these relevant temperature regimes such as that of the light water reactor (nominally 300 $^{\circ}\text{C}$.) However, based on the known irradiation-induced swelling, microstructural development, and annealing of SiC [10] at those temperatures significant stored energy likely exists. Utilizing the data of Fig. 3 and noting that a linear relationship exists between stored energy and lattice strain (swelling) it is straight-forward to estimate the stored energy content for a saturated level of swelling as a function of SiC anywhere in the point defect regime. This is provided in Fig. 8 assuming the stored energy release data from the current work and the known saturation swelling as a function of temperature from the literature [23]. For comparison, Fig. 8 compares the relative stored energy in SiC to that of graphite as presented by Kelly for typical nuclear graphite [7]. As evident from the figure, the relative stored energy for graphite rapidly diminishes above ~ 200 $^{\circ}\text{C}$ associated with highly accelerated correlated defect recombination. In contrast, SiC has a well-known gradual slope for recombination in the 100 - 800 $^{\circ}\text{C}$ point defect swelling and annihilation regime, suggesting a large fraction of residual stored energy may be available at these “relevant” elevated temperatures.

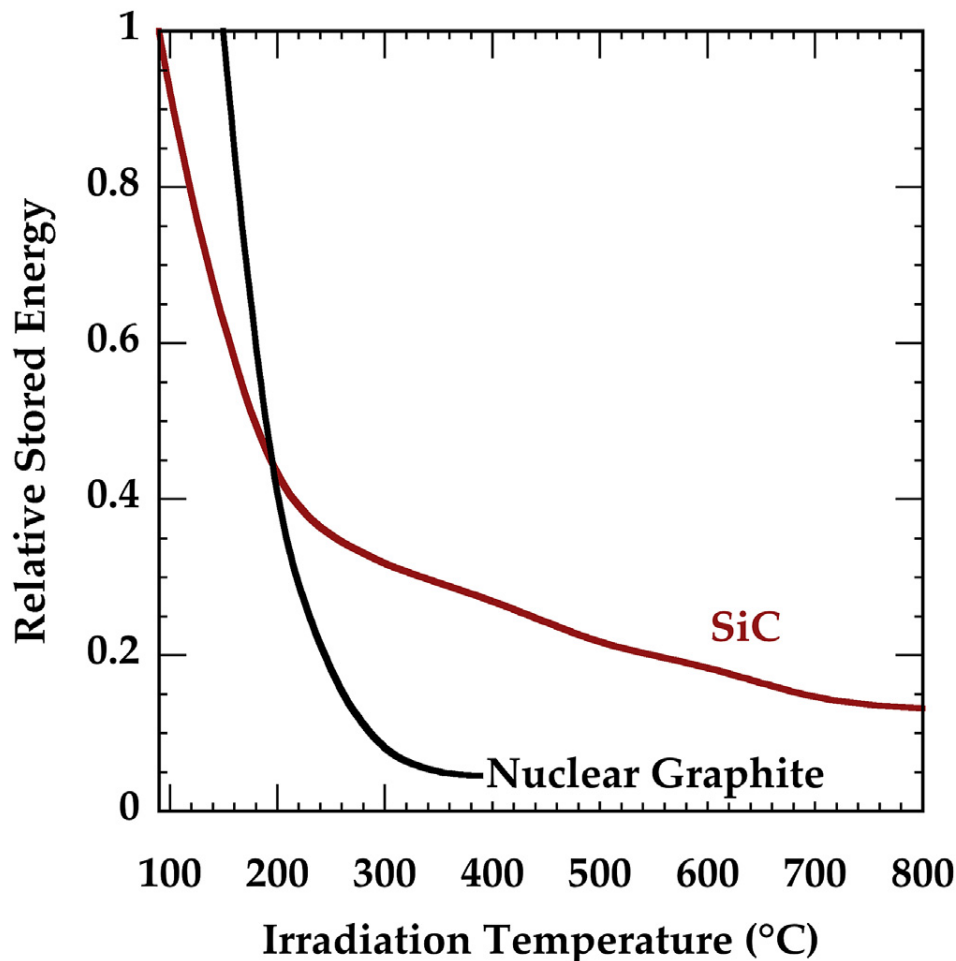


Fig. 8. Comparison of relative stored energy of pure SiC and nuclear graphite as a function of irradiation temperature.

5. Conclusions

The stored energy release in highly pure silicon carbide irradiated near 60 °C from relatively low dose in a mixed spectrum nuclear reactor to and well beyond the critical dose for amorphization has been measured. Within the limitation of the current data-set the following observations are made:

- 1) Cubic silicon carbide, which undergoes more than 7.6% isotropic crystalline strain and equivalent macroscopic swelling released 1390 J/g stored energy upon annealing to 700 °C. The stored energy content as a function of dose and as normalized to density change leading up to 7.6% crystalline swelling was essentially constant.
- 2) Silicon carbide was seen to undergo as much as 8.13% swelling prior to amorphization, at which point the measured macroscopic density at 2 and 20 dpa for the as-amorphized materials was essentially equivalent at 11.7%.
- 3) By extrapolation of the current data, the critical dose for amorphization at the applied dose rate of $1 \times 10^{19} \text{ n/m}^2\text{-s}$ ($E > 0.1 \text{ MeV}$), and at an irradiation temperature of 60 °C was approximately 1 dpa. Just prior to this point the extrapolated stored energy content for the crystalline SiC was $\sim 2500 \text{ J/g}$.
- 4) Above 0.1 dpa, the stored energy release measured in this work exceeds the materials' specific heat, as did that of the as amorphized materials, indicating the potential for an autocatalytic energy excursion depending on the particular nuclear application.
- 5) The stored energy content at the annealing condition of this work (700 °C, 1 h) for the as-amorphized 2 and 20 dpa materials was similar at 553 and 638 J/g.
- 6) The measured stored energy content for the as-irradiated crystalline materials are consistent with the current theory of defect recombination. This conclusion does acknowledge the relatively wide range in defect formation energies discussed in the literature and potentially also a different parsing of defects as compared to current understanding.

Acknowledgement

This work was supported by the U.S. Department of Energy, Office of Nuclear Energy under DOE Idaho Operations Office Contract DE-AC07-05ID14517 as part of a Nuclear Science User Facility experiment. The authors would like to thank the NSUF office for enabling this research as well as the members of the Low Activation Materials Development Laboratory (LAMDA) at ORNL and in particular Wallace Porter for their experimental support. The Principal Investigator was supported through a Department of Energy Office of Fusion Energy Sciences, Project Number 79446.

References

- [1] E. Fermi, Report for Month Ending December 15, 1942, Physics Division, USAER Report CP-387, University of Chicago, December 1942. Nov. 26.
- [2] J.W.H. Simmons, Radiation Damage in Graphite, Pergamon Press, 1965.
- [3] R. Taylor, K.E. Gilchrist, L.J. Poston, *J. Phys. Chem. Solid.* 30 (1969) 2251-2267.
- [4] W. Primak, L.H. Fuchs, P.P. Day, Radiation damage in diamond and silicon carbide, *Phys. Rev.* 103 (5) (1956) 1184-1192.
- [5] W. Primak, L.H. Fuchs, P. Day, Radiation damage in insulators, *Phys. Rev.* 92 (1953) 1064-1065.
- [6] L.L. Snead, Y. Katoh, T. Koyanagi, K. Terrani, E.D. Specht, Dimensional isotropy of 6H and 3C SiC under neutron irradiation, *J. Nucl. Mater.* 471 (2016) 92-96.
- [7] B.T. Kelly, Physics of Graphite, Applied Science Publishers, London, 1981.
- [8] L.L. Snead, S.J. Zinkle, Structural relaxation in amorphous silicon carbide, *Nucl. Instrum. Methods Phys. Res. B* 191 (2002) 497-503.
- [9] R.J. Price, Neutron irradiation-induced voids in beta-silicon carbide, *J. Nucl. Mater.* 48 (1973) 47-57.
- [10] L.L. Snead, T. Nozawa, Y. Katoh, T.S. Byun, S. Kondo, D.A. Petti, Handbook of SiC properties for fuel performance modeling, *J. Nucl. Mater.* 371 (2007) 329-377.
- [11] L.L. Snead, D. Steiner, S.J. Zinkle, Measurement of the effect of radiation damage to ceramic composite interfacial strength, *J. Nucl. Mater.* 191-194 (1992) 566-570.
- [12] L.L. Snead, S.J. Zinkle, D. Steiner, Radiation induced microstructure and mechanical property evolution of SiC/C/SiC composite material, *J. Nucl. Mater.* 191-194 (1992) 560-565.
- [13] S.J. Zinkle, L.L. Snead, Influence of irradiation spectrum and implanted ions on the amorphization of ceramics, *Nucl. Instrum. Methods Phys. Res. B* 116 (1996) 92-101.
- [14] L.L. Snead, S.J. Zinkle, J.C. Hay, M.C. Osborne, Amorphization of SiC under ion and neutron irradiation, *Nucl. Instrum. Methods Phys. Res. B* 141 (1998) 123-132.
- [15] L.L. Snead, S.J. Zinkle, J.C. Hay, M.C. Osborne, Threshold dose for amorphization of silicon carbide, in: I.M. Robertson, G.S. Was, L.W. Hobbs, T. Diaz de la Rubia (Eds.), *Microstructure Evolution during Irradiation*, Materials Research Society, Pittsburgh, 1997, pp. 595-606.
- [16] M. Ishimaru, I.-T. Bae, Y. Hirotsu, Electron-beam-induced amorphization in SiC, *Phys. Rev. B* 68 (2003), 144102-1-144102-4.
- [17] L.L. Snead, J.C. Hay, Neutron irradiation induced amorphization of silicon carbide, *J. Nucl. Mater.* 273 (1999) 213-220.
- [18] M.C. Osborne, J.C. Hay, L.L. Snead, D. Steiner, Mechanical and physical property changes of neutron irradiated CVDS silicon carbide, *J. Am. Ceram. Soc.* 82 (9) (1999) 1141-1145.
- [19] C.J. McHargue, G.C. Farlow, C.W. White, J.M. Williams, B.R. Appleton, H. Naramoto, The amorphization of ceramics by ion beams, *Mater. Sci. Eng.* 69 (1985) 123-127.
- [20] L.L. Snead, Limits on thermal conductivity and electrical resistivity of irradiated SiC, *J. Nucl. Mater.* 329-333 (2004) 524-529.
- [21] L.L. Snead, O.J. Schwartz, Advanced SiC composites for fusion applications, *J. Nucl. Mater.* 219 (1994) 3-14.
- [22] L.L. Snead, M. Osborne, K.L. More, Effects of radiation on SiC-based Nicalon fibers, *J. Mater. Res.* 10 (3) (1995) 736-746.
- [23] Y. Katoh, T. Koyanagi, J.L. McDuffee, L.L. Snead, K. Yueh, Dimensional stability and anisotropy of SiC and SiC-based composites in transition swelling regime, *J. Nucl. Mater.* 499 (2018) 471-479.

[24] A. Debelle, A. Boulle, A. Chartier, F. Gao, W.J. Weber, Interplay between atomic disorder, lattice swelling, and defect energy in ion-irradiation-induced amorphization of SiC, *Phys. Rev. B* 90 (2014) 174112.

[25] R.J. Maurer, R.C. Ruder, U. S. Atomic Energy Commission Report, April 25, 1945. CP-2889.

[26] L.H. Fuchs, W.L. Primak, The Increase in Heat Content of Diamond on Irradiation, Argonne National Laboratory Report. ANL-4466. Radiation Effects on Reactor Materials, 1950.

[27] A. Faessler, Untersuchungen zum Problem des metamikten Zustandes, *Z. Kristallogr.* 104 (1942) 81-113.

[28] H.D. Holland, J.L. Kulp, Geologic age from metamict minerals, *Science* 111 (2282) (1950) 312-313.

[29] P.F. Kerr, H.D. Holland, Differential thermal analysis of davidite, *Am. Mineral.* 36 (1951) 563-572.

[30] S.F. Kurath, Storage of energy in metamict minerals, *Am. Mineral.* 42 (1957) 91-99.

[31] G.R. Lumpkin, E.M. Foltyn, R.C. Ewing, Thermal Recrystallization of Alpharecoil Damaged Minerals of the Pyrochlore Structure Type, DOER/ER/45099- T1, October 1, 1985.

[32] S. Ellsworth, A. Novotny, R.C. Ewing, *Phys. Chem. Miner.* 21 (1994) 140-149.

[33] R.C. Ewing, Nuclear waste forms for actinides, *Proc. Natl. Acad. Sci. Unit. States Am.* 96 (1999) 3342-3429.

[34] G. Wehr, K. Boning, J. Kalus, G. Vogl, H. Wenzl, Stored energy release of solid argon after reactor irradiation at 4.6 K, *J. Phys. C Solid State Phys.* 4 (1971) 324-330.

[35] T.H. Blewitt, R.R. Coltman, C.E. Klabunde, Stored energy of irradiated copper, *Phys. Rev. Lett.* 3 (3) (1959) 132-134.

[36] R.T. Richard, R.L. Chaplin, R.R. Coltman, H.R. Kerchner, C.E. Klabunde, Stored energy recovery of irradiated copper, *Radiat. Eff. Defect Solid* 112 (1990) 161-179.

[37] T.H. Blewitt, R.R. Coltman, C.E. Klabunde, Stored energy of irradiated copper, *Phys. Rev. Lett.* 3 (3) (1959) 132-133.

[38] D. Heeger, F. Rau, P. Tischer, H. Wenzl, Erholung der gespeicherten energie und des elektrischen restwiderstands unterhalb 65K in neutronenbestrahltem kupfer, *Phys. Lett.* 21 (4) (1966) 393-394.

[39] P.G. Mayer, G. Lecomte, *J. Phys. Radium* 21 (1960) 242.

[40] G.S. Karumidze, L.S. Topchyan, B.M. Trakhbrot, Low temperature calorimetric measurement of the energy stored in a single crystal irradiated at 100K in a reactor, *Fiz. Tekh. Poluprovodn* 21 (5) (1987).

[41] J. Delaplace, J. Hillabet, J.C. Nicoud, D. Schumacher, G. Vogl, Low temperature neutron radiation damage and recovery in magnesium, *Phys. Status Solidi* 30 (1968) 119-126.

[42] J.C. Nicoud, E. Bonjour, D. Schumacher, J. Delaplace, Restauration dans le stade I du Beryllium irradie par des neutrons et par des electrons, *Phys. Lett.* 26 (6) (1968) 228-229.

[43] K. Isebeck, F. Rau, W. Schilling, K. Sonnenberg, P. Tischer, H. Wenzl, Stored energy, volume, and resistivity change in neutron irradiated aluminum, *Phys. Status Solidi B* 17 (1966) 259-268.

[44] D.A. Toktogulova, M. Gussev, O.P. Maksimkin, F.A. Garner, Influence of neutron irradiation on energy accumulation and dissipation during plastic flow and hardening of metallic polycrystals, *J. ASTM* 7 (1) (2015). JAI102175.

[45] G.H. Kinchin, M.W. Thompson, Irradiation damage and recovery in Molybdenum and tungsten, *J. Nucl. Energy* 6 (1958) 275-284.

[46] P.M. Heuer, G.Z.A. Stolarski, Stored energy in neutron-irradiated Beryllium oxide, *J. Nucl. Mater.* 19 (1966) 70-78.

[47] A. Roux, J. Elston, P. Gerard, J. Cheippe, Etude Comarative de l'energie Wigner de BeO, MgO, Al₂O₃, et SiO₂ vetreuse, *C. R. Acad. Sci. Paris t.* 272 (1971) 812-815.

[48] N. Roux, G. Hollenberg, C. Johnson, K. Noda, R. Verrall, Summary of experimental results for ceramic breeder materials, *Fusion Eng. Des.* 27 (1995) 154-166.

[49] F.P. Roberts, G.H. Jenks, C.D. Bopp, Radiation Effects in Solidified High-level Waste Part 1, Stored Energy, January 1976. BNWL- 1944 UC-70.

[50] B.G. Childs, The release of stored energy from neutron-irradiated uranium oxides, *J. Nucl. Mater.* 5 (1) (1962) 128-139.

[51] F. Cataldo, G. Angelini, Z. Revay, E. Osawa, T. Braun, Wigner energy of nanodiamond bombarded with neutrons of irradiated with gamma radiation, *Fullerenes, Nanotub. Carbon Nanostruct.* 22 (2014) 861-865.

[52] J. Li, L. Porter, S. Yip, Atomistic modeling of finite-temperature properties of crystalline beta-SiC II. Thermal conductivity and effects of point defects, *J. Nucl. Mater.* 255 (1998) 139-152.

[53] N. Swaminathan, D. Morgan, I. Szlufarska, Ab initio based rate theory model of radiation induced amorphization in SiC, *J. Nucl. Mater.* 414 (2011) 431-439.

[54] F. Gao, W.J. Weber, Cascade overlap and amorphization in 3C-SiC: defect accumulation, topological features, and disordering, *Phys. Rev. B* 66 (024106) (2002) 1-10.

[55] D. Shrader, S.M. Khalil, T. Gerczak, T.R. Allen, A.J. Heim, I. Szlufarska, D. Morgan, Ag diffusion in cubic silicon carbide, *J. Nucl. Mater.* 408 (2011) 257-271.

[56] D. Shrader, I. Szlufarska, D. Morgan, Cs diffusion in cubic silicon carbide, *J. Nucl. Mater.* 421 (1e3) (2011) 89-96.

[57] M. Bockstedte, A. Mattausch, O. Pankratov, Ab initio study of the migration of intrinsic defects in 3C-SiC, *Phys. Rev. B* 68 (2003), 205201-1-17.

[58] T. Liao, G. Roma, Stability of neutral silicon interstitials in 3C- and 4H-SiC: a first-principles study, *Defect Diffusion Forum* 283e286 (2009) 74-83.

[59] J. Li, L.J. Porter, S. Yip, Atomistic modeling of finite-temperature properties of crystalline b-SiC; II. Thermal conductivity and effects of point defects, *J. Nucl. Mater.* 255 (1998) 139-152.

[60] N. Swaminathan, P. Kamenski, D. Morgan, I. Szlufarska, Effects of grain size and grain boundaries on defect production in nanocrystalline 3C-SiC, *Acta Mater.* 58 (2010) 2843.

[61] W.J. Weber, Models and mechanisms of irradiation-induced amorphization in ceramics, *Nucl. Instrum. Methods Phys. Res. B* 166e167 (2000) 98-106.

[62] M.L. Swanson, J.R. Parsons, C.W. Hoelke, *Radiation Effects in Semiconductors*, Gordon and Breach, New York, 1971.

[63] J.A. Edmond, R.F. Davis, S.P. Withrow, K.L. More, Ion implantation in beta-SiC: effect of channeling direction and critical energy for amorphization, *J. Mater. Res.* 3 (2) (1988) 321-328.

[64] L.L. Snead, S.J. Zinkle, W.S. Eatherly, D.K. Hensley, N.L. Vaughn, J.W. Jones, Dose rate dependence of the amorphization of silicon carbide, in: S.J. Zinkle, G.E. Lucas, R.C. Ewing, J.S. Williams (Eds.), *Microstructural Processes in Irradiated Materials*, Materials Research Society, Boston MA, 1998, pp. 165-170.

[65] W.J. Weber, N. Yu, L.M. Wang, N.J. Hess, Temperature and dose dependence of ion-beam-induced amorphization in alpha-SiC, *J. Nucl. Mater.* 244 (1997) 258-265.

[66] H. Inui, H. Mori, H. Fujita, Electron irradiation induced crystalline-amorphous transition in ceramics, *Acta Metall.* 37 (5) (1989) 1337-1342.

[67] H. Inui, H. Mori, H. Fujita, Electron-irradiation-induced crystalline to amorphous transition in alpha-SiC single-crystals, *Phil. Mag. B* 61 (1) (1990) 107-124.

- [68] H. Inui, H. Mori, A. Suzuki, H. Fujita, Electron-irradiation-induced crystallineto- amorphous transition in beta-SiC single-crystals, *Phil. Mag. B* 65 (1) (1992) 1-14.
- [69] J.M. Constantini, X. Kerbiriou, M. Sauzay, L. Thome, Ion-beam modification of mechanical and dimensional properties of silicon carbide, *J. Phys. Appl. Phys.* 45 (2012) 465301.
- [70] J.B. Wallace, L.B. Bayu-Aji, L. Shao, S.O. Kucheyev, Time constant of defect relaxation in ion-irradiated 3C-SiC, *Appl. Phys. Lett.* 106 (2015) 202102.